Received: 20 March 2023 | Revised: 9 April 2023 | Accepted: 11 April 2023

DOI: 10.1002/pol.20230174

RESEARCH ARTICLE

JOURNAL OF POLYMER SCIENCE WILEY

Synthesis and design of hypercrosslinked porous organic frameworks containing tetraphenylpyrazine unit for high-performance supercapacitor

Mohsin Ejaz[1] | **Mohamed Gamal Mohamed**[1,2] | **Wan-Chun Chang**[1] | **Shiao-Wei Kuo**[1,3]

[1]Department of Materials and Optoelectronic Science, College of Semiconductor and Advanced Technology Research, Center for Functional Polymers and Supramolecular Materials, National Sun Yat-Sen University, Kaohsiung, Taiwan

[2]Chemistry Department, Faculty of Science, Assiut University, Assiut, Egypt

[3]Department of Medicinal and Applied Chemistry, Kaohsiung Medical University, Kaohsiung, Taiwan

Correspondence
Mohamed Gamal Mohamed and Shiao-Wei Kuo, Department of Materials and Optoelectronic Science, College of Semiconductor and Advanced Technology Research, Center for Functional Polymers and Supramolecular Materials, National Sun Yat-Sen University, Kaohsiung, 804, Taiwan.
Email: mgamal.eldin12@yahoo.com; kuosw@faculty.nsysu.edu.tw

Abstract

Human society faces significant environmental challenges due to the rapid production and consumption of fossil fuels. Therefore, developing effective and environmentally friendly methods of generating and storing energy is essential. Hypercrosslinked polymers (HPPs) have become increasingly popular due to their diverse preparation methods, simple functionalization, large specific surface area, low cost, mild reaction conditions, high chemical and thermal stability, and small size. We synthesized two hypercrosslinked porous organic polymers using Friedel-Crafts reactions of 2,3,5,6-tetraphenyl pyrazine (Pyra) with 4,4′-bis(chloromethyl)biphenyl (BP), and dimethoxymethane (DDM), resulting in Pyra-BP-HPP and Pyra-DDM-HPP, respectively. The chemical structures and thermal stability of these polymers were confirmed through solid-state ^{13}C NMR, FTIR, and TGA. The surface area of Pyra-BP-HPP and Pyra-DDM-HPP was determined to be 984 and 435 $m^2\ g^{-1}$, respectively, with micro and mesoporous structures present. Pyra-BP-HPP displayed a high specific capacitance of 94 $F\ g^{-1}$ at 1 $A\ g^{-1}$, with a capacity retention of 95% after 2000 cycles, which can be attributed to its larger surface area, microporosity, and abundance of electron-rich phenyl rings when compared to Pyra-DDM-HPP.

KEYWORDS

Friedel–crafts reaction, hypercrosslinked porous organic polymers, supercapacitors, tetraphenyl pyrazine

1 | INTRODUCTION

The dramatic rise in carbon dioxide emissions has caused serious problems such as global warming, resource shortages, and environmental degradation.[1–5] To mitigate these issues, various measures are being taken to reduce CO_2 production. One promising solution is the development of low-cost and eco-friendly systems that can provide long-term benefits to society, such as batteries and supercapacitors (SCs).[5,6] Supercapacitors offer several advantages, including high energy density, excellent durability, fast charge/discharge rates, and high stability, making them a practical solution to the energy shortage crisis.[7–12] However, their energy density is still lower than other rechargeable batteries, limiting their overall energy storage capacity.[13,14] To address this limitation, researchers are exploring ways to improve the performance of SCs and develop multifunctional materials with

high surface areas, adjustable porous morphologies, and highly conductive frameworks to increase demand for SCs.[15–22] The absence of any chemical processes, such as redox reactions, and the lack of charge transport between electrodes and electrolytes characterize the behavior of electric double-layer capacitors (EDLCs). The charge in EDLCs is stored in a non-faradaic manner. In contrast, pseudocapacitance involves the occurrence of chemical redox reactions and faradaic charge storage. The coexistence of both EDLC and pseudocapacitance behavior indicates the presence of both faradaic and non-faradaic characteristics. This combination of characteristics has a positive effect on the capacitance and stability of the system.[15–22]

Hypercrosslinked porous polymers (HPPs) are a type of multifunctional porous organic polymer (POP) that offers several advantages, including simple functionalization, high surface area, controlled reaction conditions, various synthetic routes, and good thermal stability.[17–33] The Friedel-Crafts reaction is a common method for producing HPPs, as it allows for the quick establishment of linkages and the creation of a strongly crosslinked framework with enhanced porosity geometry.[34–44] A wide range of aromatic monomers can produce polymer frameworks with different porosities or introduce specific functionalities that increase the surface area and other desirable characteristics of the materials.[44] Hypercrosslinked porous organic frameworks (HPPs) offer a multitude of benefits that make them superior to other materials, such as metal oxides, carbon, and composites for supercapacitor applications. These advantages include a high surface area and tunable porosity, which enhance ion transportation and increase their specific capacitance. Additionally, HPPs are cost-effective to prepare, unlike metal oxides. They also offer significant energy density, are environmentally friendly, and are lightweight, giving them an edge over metal oxides. The combination of these factors makes HPPs an attractive candidate for supercapacitor applications.[45–48] To enhance their supercapacitor properties, researchers have introduced different building blocks or heteroatoms (N, S, P, and B) into their frameworks to increase surface area and conductivity.[49,50] Several studies have investigated the performance of HPPs in energy storage applications. For example, Kim et al. prepared a xylene-based hypercrosslinked polymer using the Friedel-Crafts reaction and observed a specific capacitance of 242.5 F g^{-1} at 1.25 A g^{-1}.[51] The Vinodh group synthesized anthracene-linked HPPs with good microporosity, a surface area of 928 m^2 g^{-1}, and a specific capacitance of 206.4 F g^{-1}.[52] Mohamed et al. prepared tetraphenylethene-centered HPPs with a specific capacitance of 110 F g^{-1} at 0.5 A g^{-1} and a surface area of 1000 m^2 g^{-1}.[53] Sun et al. synthesized carbazole-linked HPPs with a specific capacity of 23 F g^{-1} at 0.1 mA cm^{-2}.[54]

Over the past few years, there has been a surge of interest in tetraphenylpyrazine (TPP) and its derivatives as a novel type of heterocyclic-based luminogens with aggregation-induced emission (AIE) properties.[45,55,56] These compounds have inherent benefits such as exceptional stability, the ability to tune emission color, easy synthetic protocols, and effortless structural modification.[45,55,56] The energy storage potential of hypercrosslinked porous polymers (HPPs) containing the heterocyclic derivative tetraphenylpyrazine (Pyra) has not been thoroughly studied. In this study, we aimed to address this gap by synthesizing two different HPPs: Pyra-BP-HPP and Pyra-DDM-HPP. Both were obtained through the Friedel-Crafts reaction of 2,3,5,6-tetraphenyl pyrazine with 4,4′-bis(chloromethyl)biphenyl and dimethoxymethane, respectively, in the presence of $FeCl_3$, methane sulfonic acid, and 1,2-dichlorobenzene. These HPPs were found to have high surface areas and porosities, making them suitable as active electrode materials for supercapacitors. The chemical structures, porosities, thermal stabilities, and electrochemical performances of these HPPs are discussed in detail below.

2 | EXPERIMENTAL SECTION

2.1 | Materials

4,4′-Bis(chloromethyl)biphenyl (BP), dimethoxymethane (DDM), methanesulfonic acid, anhydrous ferric chloride ($FeCl_3$), 1,2-dichlorobenzene, acetic acid (AcOH), acetic anhydride (Ac_2O), ammonium acetate (CH_3COONH_4) and benzoin were purchased from Sigma Aldrich. Acetone, Dichloromethane (DCM), and tetrahydrofuran (THF) were ordered from Aldrich.

2.2 | Synthesis of tetraphenylpyrazine (Pyra)

A 50-mL round bottom flask was filled with 4 g of BZ (18.90 mmol), 2.73 mL of Ac_2O (28.30 mmol), 4.40 g of CH_3COONH_4 (56.60 mmol), and 150 mL of AcOH. The mixture was cooled to room temperature and filtered after 3.5 hours of refluxing. Pyra monomer (Scheme S1) was produced as a white solid by recrystallizing the crude products in acetic acid. FTIR (cm^{-1}, Figure S1): 3019 (CH aromatic), 1631 (C═N). ^1H NMR ($CDCl_3$, ppm, Figure S2a): 7.64 (m, 8H), 7.36 (m, 12H). ^{13}C NMR ($CDCl_3$, ppm, Figure S2b): 148.0–129.4.

2.3 | Synthesis of Pyra-BP-HPP

In a 150-mL flask, 2,3,5,6-tetraphenylpyrazine (0.7 g, 1.82 mmol), 4,4′-bis(chloromethyl)biphenyl (2.73 g, 10.92 mmol), $FeCl_3$ (1.77 g, 10.91 mmol), methanesulfonic acid (2.12 mL, 32.77 mmol) and 1,2-dichlorobenzene (30 mL) were mixed, stirred, and heated under N_2 at 140 °C for 72 h. The insoluble products were filtered and washed several times with THF, methanol, DCM, and acetone to afford Pyra-BP-HPP as a brown powder (Scheme 1A).

2.4 | Synthesis of Pyra-DDM-HPP

In a 150-mL flask, 2,3,5,6-tetraphenylpyrazine (0.7 g, 1.82 mmol), dimethoxymethane (0.83 g, 10.91 mmol), $FeCl_3$ (1.77 g, 10.91 mmol), methanesulfonic acid (2.12 mL, 32.77 mmol), and 1,2-dichlorobenzene (30 mL) were mixed, stirred, and heated under N_2 at 140 °C for 72 hours. The insoluble products were filtered and washed several times with THF, methanol, DCM, and acetone to afford Pyra-DDM-HPP as a brown powder (Scheme 1B).

3 | RESULT AND DISCUSSION

3.1 | Synthesis and characterization of Pyra-BP-HPP and Pyra-DDM-HPP

We synthesized two porous HPPs, Pyra-BP-HPP and Pyra-DDM-HPP, using the Friedel-Crafts reaction method, as shown in Scheme 1. First, we synthesized the Pyra monomer by reacting BZ with CH_3COONH_4 in the presence of AcOH at 90 °C for 24 h (Scheme S1). To create Pyra-BP-HPP, we reacted 2,3,5,6-tetraphenylpyrazine with 4,4′-bis(chloromethyl)biphenyl, and for Pyra-DDM-HPP, we reacted 2,3,5,6-tetraphenylpyrazine with dimethoxymethane. Both reactions were carried out in the presence of $FeCl_3$, methanesulfonic acid, and 1,2-dichlorobenzene, and the mixture was stirred and heated under N_2 at 140 °C for 48 h (Scheme 1).

We used FTIR spectroscopy to identify the functional groups in both Pyra-BP-HPP and Pyra-DDM-HPP. The peaks of C═N (imino) and C═C aromatics were observed at 1705 cm^{-1} and 1603 cm^{-1}, respectively, and the aliphatic (C-H) group centered at 2918 cm^{-1} was present in both materials (Figure 1A). The solid-state ^{13}C NMR of both materials also confirmed the presence of C═N at 178 ppm, while the signal for aromatic carbons was observed at 128–139 ppm and for aliphatic carbons at 38 ppm (Figure 1B). The presence of aliphatic linkers confirmed the successful synthesis of both materials through the Friedel-Crafts reaction. We measured the thermal stability of both Pyra-BP-HPP and Pyra-DDM-HPP using thermogravimetric (TGA) analysis (Figure 1C). The T_{d5}, T_{d10}, and char yield were observed as 195 °C, 233 °C, and 69.74 wt% for Pyra-BP-HPP, while 299 °C, 372 °C, and 56.5 wt% for Pyra-DDM-HPP, respectively. Pyra-BP-HPP showed higher thermal stability than Pyra-DDM-HPP, which can be attributed to its higher crosslinking density. We analyzed the nature of both materials using powder X-ray diffraction (PXRD) studies,

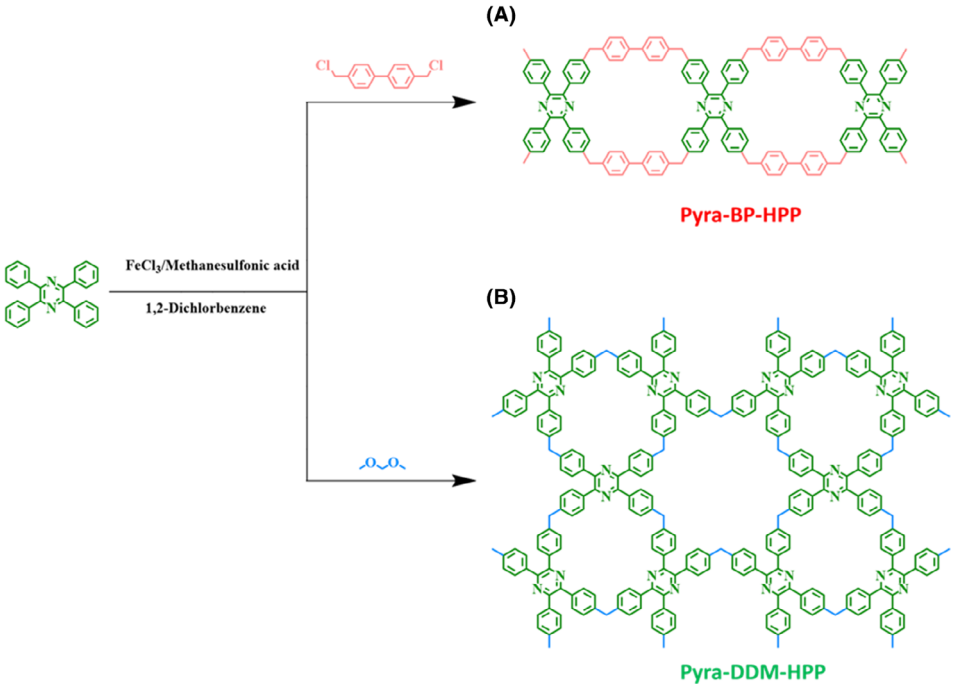

SCHEME 1 Synthesis of (A) Pyra-BP-HPP and (B) Pyra-DDM-HPP from Pyra moiety through Friedel–crafts reaction.

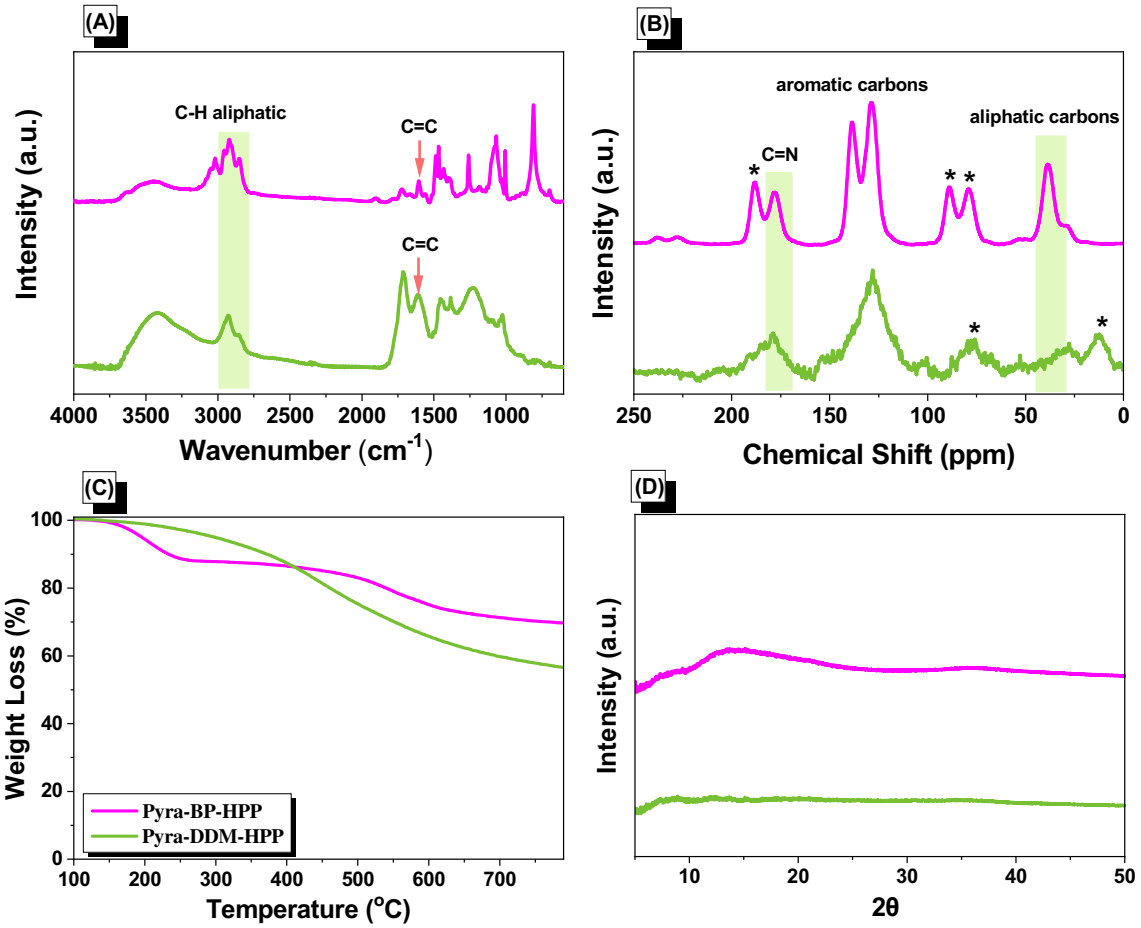

FIGURE 1 (A) FT-IR; (B) Solid state ^{13}C NMR; (C) TGA; and (D) XRD of Pyra-BP-HPP and Pyra-DDM-HPP.

which showed that both materials had broad peaks demonstrating their amorphous characteristics (Figure 1D).

The N_2 sorption at 77 K was utilized to analyze the porosities of Pyra-BP-HPP and Pyra-DDM-HPP. As per UPAC standards, type I isotherms were observed for both Pyra-BP-HPP and Pyra-DDM-HPP (Figure 2A,B), with an S_{BET} of 984 and 435 $m^2\ g^{-1}$, respectively. The rapid N_2 absorption uptake in the low and high-pressure zones indicated the existence of microporous and mesoporous structures in both Pyra-BP-HPP and Pyra-DDM-HPP. Using non-local density functional theory, the pore size of Pyra-BP-HPP and Pyra-FDA-HPP was observed as 1.45 and 1 nm, respectively (Figure 2C,D). The pore volumes were 0.73 and 0.31 $cm^{-3}\ g^{-1}$ for Pyra-BP-HPP and Pyra-DDM-HPP, respectively.

The SEM and TEM analysis confirmed the morphologies of porous Pyra-BP-HPP and Pyra-DDM-HPP, as shown in Figure 3A–F. The SEM analysis showed spherical agglomerated particles for both Pyra-BP-HPP and Pyra-DDM-HPP. The TEM analysis revealed spherical particles for Pyra-BP-HPP (Figure 3C) and tiny bright and dark regions for Pyra-DDM-HPP (Figure 3F), demonstrating its high porosity.

The energy-dispersive X-ray (EDX) and element mapping studies of the SEM images demonstrated the presence of C and N atoms in both Pyra-BP-HPP and Pyra-DDM-HPP (Figure 4A–F).

3.2 | Electrochemical analysis of the Pyra-BP-HPP and Pyra-DDM-HPP

Our study involved cyclic voltammetry (CV) and galvanostatic (GCD) analyses within the potential range from 0 to −1.0 V to assess the electrochemical performance of our synthesized HPPs and evaluate their suitability as energy storage electrode materials. To obtain the CV traces of Pyra-BP-HPP and Pyra-DDM-HPP, we used different scan rates, presented in (Figure 5A,B). At both low and high sweep rates, we observed rectangular humped CV curves for Pyra-BP-HPP and Pyra-DDM-HPP (Figure 5A,B), indicating that these materials are stable

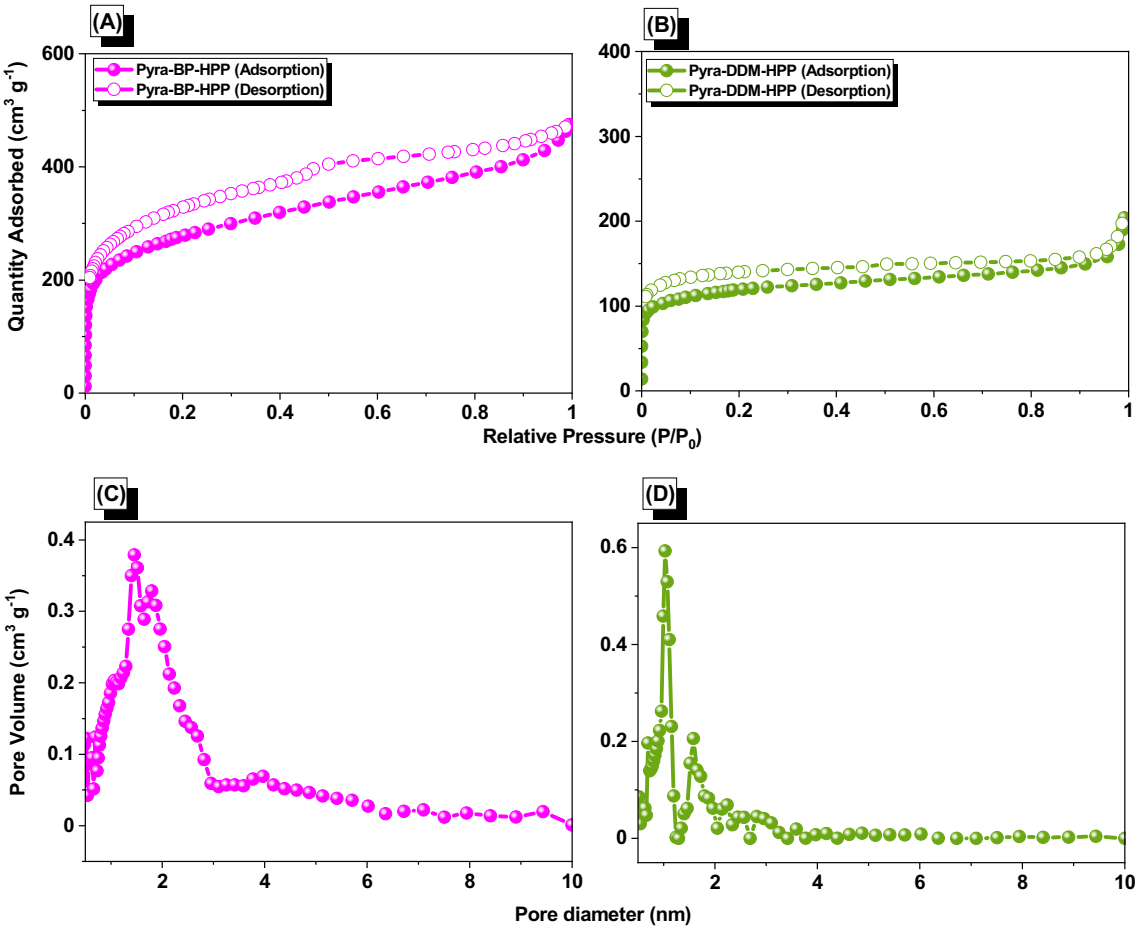

FIGURE 2 (A, B) N_2 isotherms curves and (C, D) pore diameter of the (A, C) Pyra-BP-HPP and (B, D) Pyra-DDM-HPP.

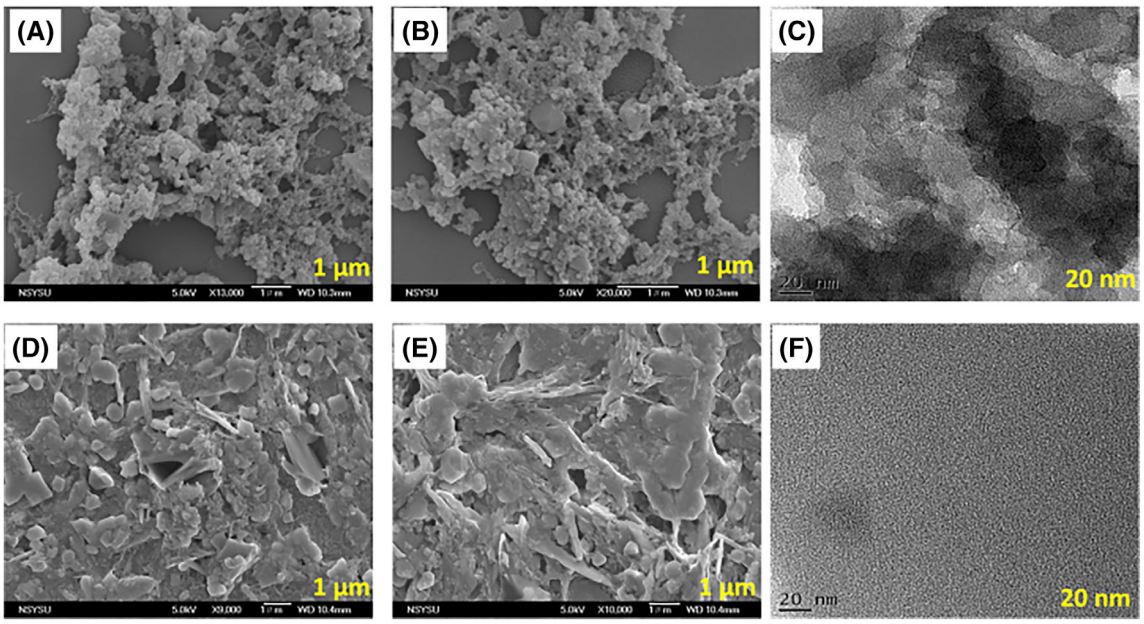

FIGURE 3 SEM (A, B, D, E) and TEM (C, F) images of Pyra-BP-HPP (A–C) and Pyra-DDM-HPP (D–F).

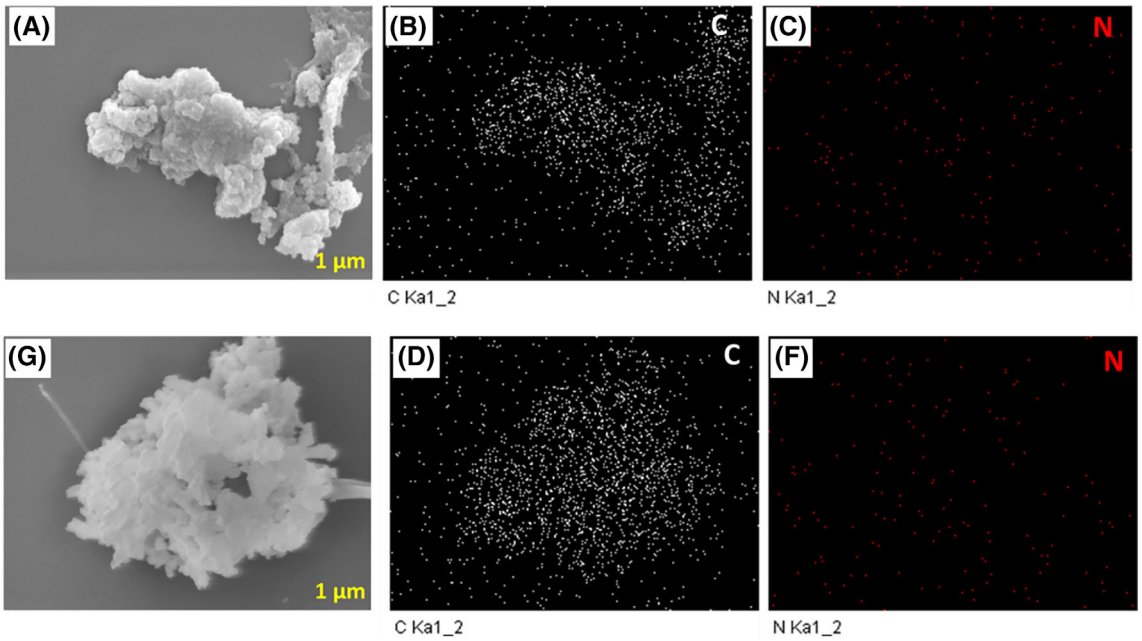

FIGURE 4 EDS-SEM mapping of Pyra-BP-HPP (A–C) and Pyra-DDM-HPP (D–F).

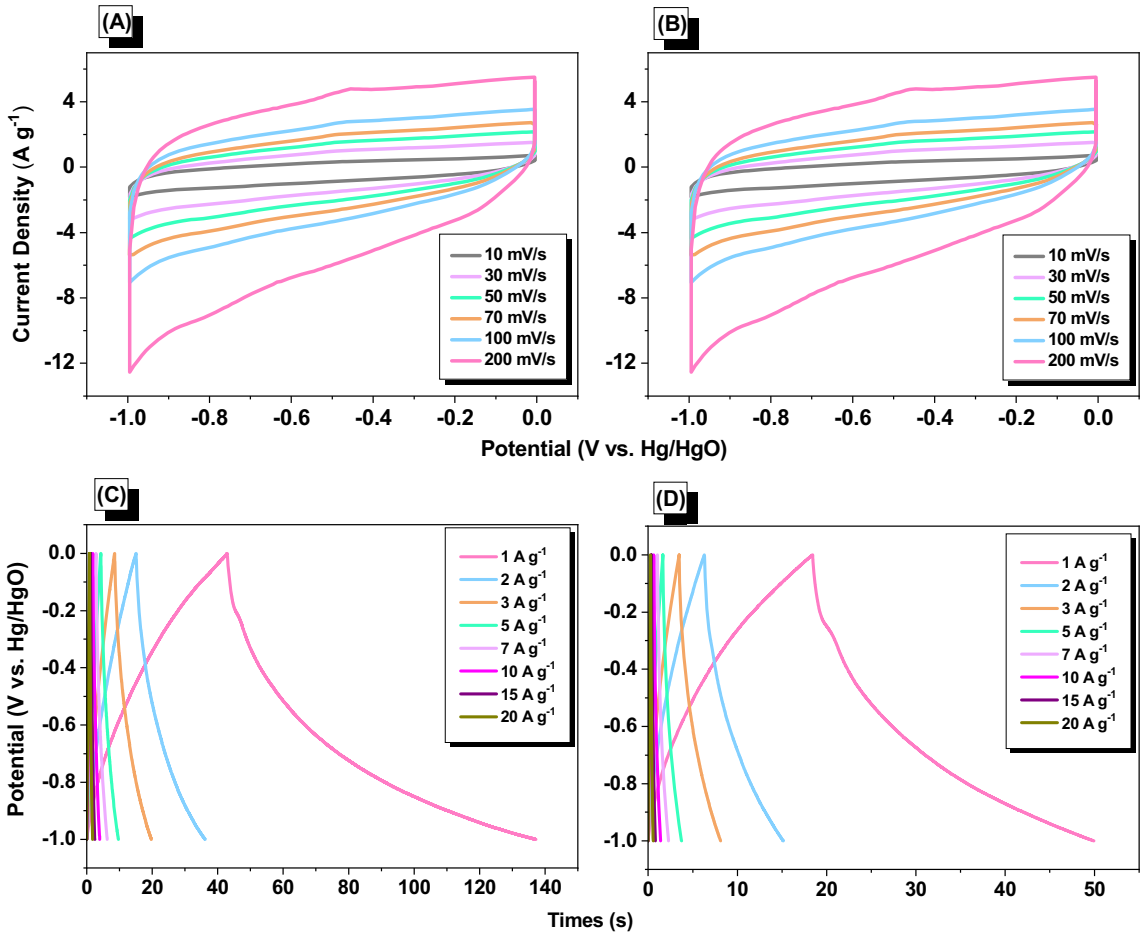

FIGURE 5 (A, B) CV and (C, D) *G* curves of (A, C) Pyra-BP-HPP and (B, D) Pyra-DDM-HPP.

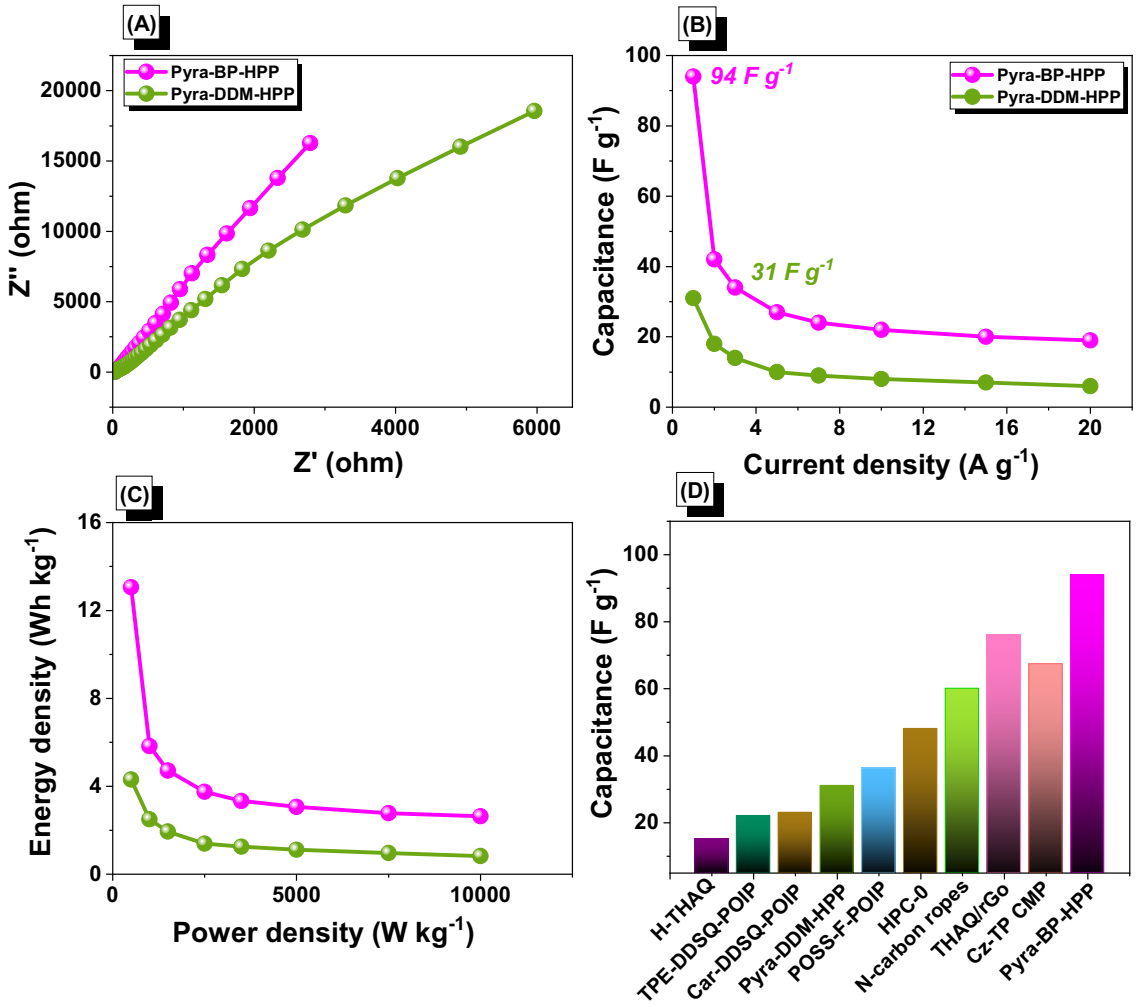

FIGURE 6 (A) EIS, (B) specific capacity, (C) Ragone profiles, (D) comparison of supercapacitor performance with other porous materials for Pyra-BP-HPP and Pyra-DDM-HPP.

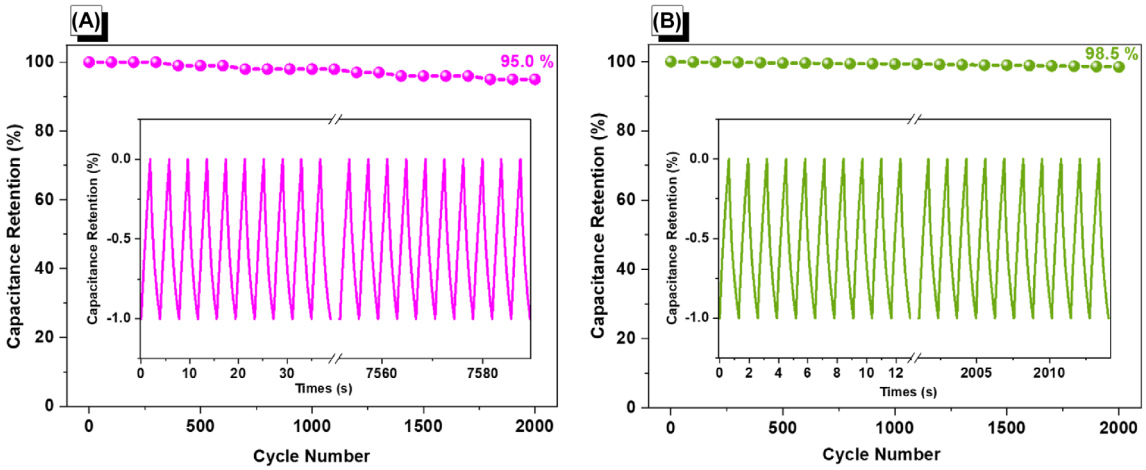

FIGURE 7 Stability at 2000 cycles for (A) Pyra-BP-HPP and (B) Pyra-DDM-HPP.

and exhibit capacitance arising from EDLC and pseudo-capacitance behavior.[57–59] Moreover, we conducted GCD measurements for Pyra-BP-HPP and Pyra-DDM-HPP at various current densities (ranging from 20 to 1 A g^{-1}) (Figure 5C,D). The resulting GCD curves were triangular in shape, which is characteristic of pseudocapacitive and

EDLC behavior. Notably, the discharge times for both Pyra-BP-HPP and Pyra-DDM-HPP electrode materials were significantly longer than the charging times, indicating improved capacitance.

In addition to cyclic voltammetry and galvanostatic analysis, we also measured the electrochemical impedance spectroscopy (EIS) of both Pyra-BP-HPP and Pyra-DDM-HPP. Our results revealed that Pyra-BP-HPP had a smaller internal resistance than Pyra-DDM-HPP, indicating superior electrochemical performance (Figure 6A). At 1 A g^{-1}, Pyra-BP-HPP exhibited a specific capacitance of 94 F g^{-1}, while Pyra-DDM-HPP had a specific capacitance of 31 F g^{-1} (Figure 6B). Even at a higher current density of 20 A g^{-1}, Pyra-BP-HPP still had a higher specific capacitance of 19 F g^{-1} compared to Pyra-DDM-HPP (6 F g^{-1}), indicating a significant difference in performance between the two materials. The excellent electrochemical characteristics of Pyra-BP-HPP could be attributed to its larger surface area, microporosity, and abundance of electron-rich phenyl rings compared to Pyra-DDM-HPP. These characteristics would facilitate the transportation of electrolytes to the electrode surface, enhancing mass mobility and electrochemical performance.[60–63] However, as the current density increased from 0.5 to 20 A g^{-1}, the specific capacitance of both materials decreased, likely due to a lack of time for ion mobility. Additionally, we found that the energy density of Pyra-BP-HPP was higher than that of Pyra-DDM-HPP, with values of 13.06 W h kg^{-1} and 4.31 W h kg^{-1}, respectively (Figure 6C). Overall, the electrochemical performance of both Pyra-BP-HPP and Pyra-DDM-HPP electrode materials (Figure 6D) was superior to that of other porous materials.[64–69]

To assess the long-term stability of Pyra-BP-HPP and Pyra-DDM-HPP, we conducted cycling stability tests at 10 A g^{-1} for 2000 cycles, as illustrated in Figure 7A,B. Both Pyra-BP-HPP and Pyra-DDM-HPP exhibited high capacity retention, with Pyra-BP-HPP retaining 95% of its initial capacitance and Pyra-DDM-HPP retaining 98% of its initial capacitance. These results suggest that both electrode materials have excellent cycling stability, even under high current densities.

4 | CONCLUSION

We synthesized two tetraphenyl pyrazine-linked HPPs, Pyra-BP-HPP, and Pyra-DDM-HPP, using Pyra monomer, BP, and DMM as external crosslinker reagents through Friedel–Crafts reaction (as shown in Scheme 1). Pyra-BP-HPP exhibited excellent electrochemical performance, owing to its large surface area, microporosity, and abundance of electron-rich phenyl rings compared to Pyra-DDM-HPP. At 1 A g^{-1}, Pyra-BP-HPP and Pyra-DDM-HPP showed a specific capacitance of 94 and 31 F g^{-1}, respectively, and both materials had capacity retention of 95% and 98% after 2000 cycles, indicating good cycling stability. These findings suggest that these electroactive materials could be a potential candidate for energy storage device applications.

ACKNOWLEDGMENTS

This study was supported financially by the Ministry of Science and Technology, Taiwan, under contracts NSTC110-2811-E-110-002 and NSTC-111-2223-E-110-004.

CONFLICT OF INTEREST STATEMENT

The authors declare no conflict of interest.

DATA AVAILABILITY STATEMENT

The data that support the findings of this study are available from the corresponding author upon reasonable request.

ORCID

Mohamed Gamal Mohamed https://orcid.org/0000-0003-0301-8372

Shiao-Wei Kuo https://orcid.org/0000-0002-4306-7171

REFERENCES

[1] M. G. Mohamed, T. H. Mansoure, M. M. Samy, Y. Takashi, A. A. K. Mohammed, T. Ahamad, S. M. Alshehri, J. Kim, B. M. Matsagar, *Molecules* **2025**, *2022*, 27.

[2] Y. Liao, H. Wang, M. Zhu, A. Thomas, *Adv. Mater.* **2018**, *30*, 1705710.

[3] N. N. Loganathan, V. Perumal, B. R. Pandian, R. Atchudan, T. N. J. I. Edison, M. Ovinis, *Journal of Energy Storage* **2022**, *49*, 104149.

[4] M. G. Mohamed, S. V. Chaganti, M. S. Li, M. M. Samy, S. U. Sharma, J. T. Lee, M. H. Elsayed, H. H. Chou, S. W. Kuo, *ACS Appl. Energy Mater.* **2022**, *5*, 6442.

[5] S. Zheng, Q. Li, H. Xue, H. Pang, Q. Xu, *Natl Sci Rev* **2020**, *7*, 305.

[6] C. Liu, Y. Bai, W. Li, F. Yang, G. Zhang, H. In Pang, *Am. Ethnol.* **2022**, *61*, 202116282.

[7] S. Liu, L. Kang, J. Henzie, J. Zhang, J. Ha, M. A. Amin, M. S. A. Hossain, S. C. Jun, Y. Yamauchi, *ACS Nano* **2021**, *15*, 18931.

[8] S. Liu, L. Kang, J. Zhang, E. Jung, S. Lee, S. C. Jun, *Energy Storage Mater* **2022**, *32*, 167.

[9] M. G. Mohamed, H. Y. Hu, M. Madhu, M. M. Samy, I. M. A. Mekhemer, W. L. Tseng, H. H. Chou, S. W. Kuo, *Eur. Polym. J.* **2023**, *189*, 111980.

[10] S. Liu, L. Kang, J. Zhang, S. C. Jun, Y. Yamauchi, *ACS Energy Lett.* **2021**, *6*, 4127.

[11] Z. Xu, S. Sun, Y. Han, Z. Wei, Y. Cheng, S. Yin, W. Cui, *Appl. Energy Mater.* **2020**, *3*, 5393.

[12] S. Liu, L. Kang, J. Hu, E. Jung, J. Zhang, S. C. Jun, Y. Yamauchi, *ACS Energy Lett.* **2021**, *6*, 3011.

[13] M. G. Mohamed, M. M. Samy, T. H. Mansoure, C. J. Li, W. C. Li, J. H. Chen, K. Zhang, S. W. Kuo, *Int. J. Mol. Sci.* **2022**, *23*, 347.
[14] M. G. Mohamed, S. Y. Chang, M. Ejaz, M. M. Samy, A. O. Mousa, S. W. Kuo, *Molecules* **2023**, *28*, 3234.
[15] Y. Dong, J. Zhu, Q. Li, S. Zhang, H. Song, D. Jia, *J. Mater. Chem. A* **2020**, *8*, 21930.
[16] M. M. Samy, M. G. Mohamed, S. W. Kuo, *Polymers* **2023**, *15*, 1095.
[17] M. M. Samy, M. G. Mohamed, S. U. Sharma, S. V. Chaganti, J. T. Lee, S. W. Kuo, *J. Taiwan Inst. Chem. Eng.* **2023**, 104750. https://doi.org/10.1016/j.jtice.2023.104750
[18] Y. S. Ye, M. G. Mohamed, C. W. Chen, S. W. Kuo, *J. Mater. Chem. A* **2023**. https://doi.org/10.1039/D2TA09232H
[19] Y. Tao, T. X. Wang, X. Ding, B. H. Han, *J. Polym. Sci.* **2024**, *62*(8), 1569. https://doi.org/10.1002/pol.20220601
[20] M. M. Samy, M. G. Mohamed, S. W. Kuo, *Compos Sci Technol.* **2020**, *199*, 108360.
[21] M. M. Samy, M. G. Mohamed, S. U. Sharma, S. V. Chaganti, T. H. Mansoure, J. T. Lee, T. Chen, S. W. Kuo, *Polymer* **2023**, *264*, 125541.
[22] M. G. Mohamed, E. C. Atayde Jr., B. M. Matsagar, J. Na, Y. Yamauchi, K. C. W. Wu, S. W. Kuo, *J. Taiwan Inst. Chem. Eng.* **2020**, *112*, 180.
[23] M. G. Mohamed, T. C. Chen, S. W. Kuo, *Macromolecules* **2021**, *54*, 5866.
[24] M. G. Mohamed, A. F. M. EL-Mahdy, M. G. Kotp, S. W. Kuo, *Mater. Adv* **2022**, *3*, 707.
[25] W. T. Chung, I. M. A. Mekhemer, M. G. Mohamed, A. M. Elewa, A. F. M. EL-Mahdy, H. H. Chou, S. W. Kuo, K. C. W. Wu, Coord, *Chem. Rev.* **2023**, *483*, 215066.
[26] M. M. Samy, I. M. A. Mekhemer, M. G. Mohamed, M. H. Elsayed, K. H. Lin, Y. K. Chen, T. L. Wu, H. H. Chou, S. W. Kuo, *Chem. Eng. J.* **2022**, *446*, 137158.
[27] M. G. Mohamed, W. C. Chang, S. W. Kuo, *Macromolecules* **2022**, *55*, 7879.
[28] M. P. Tsyurupa, V. A. Davankov, *React. Funct. Polym.* **2006**, *66*, 768.
[29] N. Fontanals, R. M. Marce, F. Borrull, P. A. G. Cormack, *Polym. Chem.* **2015**, *6*, 7231.
[30] S. Wang, M. Tu, T. Peng, C. Zhang, T. Li, I. Hussain, J. Wang, B. Tan, *Nat. Commun.* **2019**, *10*, 676.
[31] B. Li, R. Gong, W. Wang, X. Huang, W. Zhangm, H. Li, C. Hu, B. Tan, *Macromolecules* **2011**, *4*, 2410.
[32] R. Penchah, A. Ghaemi, H. G. Gilani, *Energy Fuels* **2019**, *33*, 12578.
[33] L. Ding, H. Gao, F. Xie, W. Li, H. Bai, L. Li, *Macromolecules* **2017**, *50*, 956.
[34] T. Ratvijitvech, M. Barrow, A. I. Cooper, D. J. Adams, *Polym. Chem.* **2015**, *6*, 7280.
[35] M. G. Mohamed, X. Zhang, T. H. Mansoure, A. F. M. EL-Mahdy, C. F. Huang, M. Danko, Z. Xin, S. W. Kuo, *Polymer* **2020**, *205*, 122857.
[36] M. G. Mohamed, S. V. Chaganti, S. U. Sharma, M. M. Samy, M. Ejaz, J. T. Lee, K. Zhang, S. W. Kuo, A. C. S. Appl, *Energy Mater.* **2022**, *5*, 10130.
[37] Z. Zhan, H. Wang, Q. Huang, S. Li, X. Yi, Q. Tang, J. Wang, B. Tan, *Small* **2021**, *18*, 2105083.
[38] X. Lu, S. Shi, G. Zhu, L. Zhao, M. Wang, J. Gao, Z. Du, J. Xu, *ChemistrySelect* **2020**, *5*, 549.
[39] Q. M. Zhang, T. L. Zhai, Z. Wang, G. Cheng, H. Ma, Q. P. Zhang, Y. H. Zhao, B. Tan, C. Zhang, *Adv. Mater. Interfaces* **2019**, *6*, 1900249.
[40] M. P. Tsyurupa, V. A. Davankov, *React. Funct. Polym.* **2002**, *53*, 193.
[41] D. Zhang, L. Tao, J. Ju, Y. Wang, Q. Wang, T. Wang, *Polymer* **2015**, *60*, 234.
[42] V. A. Davankov, S. V. Rogoshin, M. P. Tsyurupa, *J. Polym. Sci., Polym. Symp.* **1974**, *47*, 95.
[43] V. A. Davankov, M. P. Tsyurupa, *React. Polym.* **1990**, *13*, 27.
[44] L. Tan, B. Tan, *Chem. Soc. Rev.* **2017**, *46*, 3322.
[45] M. G. Mohamed, M. Y. Tsai, C. F. Wang, C. F. Huang, M. Danko, L. Dai, T. Chen, S. W. Kuo, *Polymers* **2021**, *13*, 221.
[46] X. Wang, P. Mu, C. Zhang, Y. Chen, J. Zeng, F. Wang, J. X. Jiang, A. C. S. Appl, *Mater. Interfaces* **2017**, *9*, 20779.
[47] M. G. Mohamed, M. M. M. Ahmed, W. T. Du, S. W. Kuo, *Molecules* **2021**, *26*, 738.
[48] L. Wu, P. Wang, X. Chen, J. Zhang, H. Luo, *Carbon Lett.* **2022**, *32*, 849.
[49] H. Wang, Z. Li, Z. Meng, X. Guo, Y. Du, H. Yang, *New J. Chem.* **2021**, *45*, 7060.
[50] W. Zou, S. Zhang, Z. Ali, Z. Miao, Y. Abbas, W. Liu, M. Qiu, Z. Wu, *Ionics* **2022**, *28*, 3985.
[51] S. H. Kim, R. Vinodh, C. V. V. M. Gopi, V. G. R. Kummara, S. Sambasivam, I. M. Obaidat, H. J. Kim, *Mater. Lett.* **2020**, *263*, 127222.
[52] R. Vinodh, R. S. Babu, C. V. V. M. Gopi, C. Deviprasath, R. Atchudanc, L. M. Samyn, A. L. F. Barros, H. J. Kim, M. Yi, *J. Energy Storage* **2020**, *28*, 101196.
[53] M. G. Mohamed, A. F. M. EL-Mahdy, T. S. Meng, M. M. Samy, S. W. Kuo, *Polymers* **2020**, *12*, 2426.
[54] Y. Sun, G. Zhu, X. Zhao, W. Kang, M. Li, X. Zhang, H. Yang, L. Guo, B. Lin, *Sol. Energy Mater. Sol. Cells* **2020**, *215*, 110661.
[55] G. Gong, H. Wu, T. Zhang, Z. Wang, X. Li, Y. Xie, *Mater. Chem. Front.* **2021**, *5*, 5012.
[56] L. Pan, Y. Cai, H. Wu, F. Zhou, A. Qin, Z. W. B. Z. Tang, *Mater. Chem. Front.* **2018**, *2*, 1310.
[57] Q. Wang, Y. Zhang, H. Jiang, T. Hu, C. Meng, A. C. S. Appl, *Energy Mater.* **2018**, *1*, 3396.
[58] Z. Xu, S. Sun, Y. Han, Z. Wei, Y. Cheng, S. Shougen Yin, W. Cui, *ACS Appl. Energy Mater.* **2020**, *3*, 5393.
[59] G. Bhattacharya, S. J. Fishlock, J. S. Roy, A. Pritam, D. Banerjee, S. Deshmukh, S. Ghosh, J. A. McLaughlin, S. S. Roy, *Global Challenges* **2019**, *3*, 1800066.
[60] M. G. Mohamed, M. M. Samy, T. H. Mansoure, S. U. Sharma, M. S. Tsai, J. H. Chen, J. T. Lee, S. W. Kuo, A. C. S. Appl, *Energy Mater.* **2022**, *5*, 3677.
[61] C. Su, H. He, L. Xu, K. Zhao, C. Zheng, C. Zhang, *J. Mater. Chem. A* **2017**, *5*, 2701.
[62] T. H. Weng, M. G. Mohamed, S. U. Sharma, S. V. Chaganti, M. M. Samy, J. T. Lee, S. W. Kuo, A. C. S. Appl, *Energy Mater.* **2022**, *5*, 14239.
[63] M. Ejaz, M. M. Samy, Y. Ye, S. W. Kuo, M. G. Mohamed, *Int. J. Mol. Sci.* **2023**, *24*, 2501.
[64] L. Xu, R. Shi, H. Li, C. Han, M. Wu, C. P. Wong, F. Kang, B. Li, *Carbon* **2018**, *127*, 459.

[65] M. G. Mohamed, W. C. Chen, A. F. M. Mahdy, S. W. Kuo, *J. Polym. Res.* **2021**, *28*, 219.
[66] M. G. Mohamed, T. H. Mansoure, Y. Takashi, M. M. Samy, T. Chen, S. W. Kuo, *Microporous Mesoporous Mater.* **2021**, *328*, 111505.
[67] L. Wan, J. Wang, L. Xie, Y. Sun, K. Li, *ACS Appl. Mater. Interfaces* **2014**, *6*, 15583.
[68] P. Thirukumaran, A. Parven, Y. R. Lee, S. C. Kim, *J. Alloys Comp.* **2018**, *750*, 384.
[69] S. F. Saber, S. U. Sharma, J. T. Lee, A. F. M. EL-Mahdy, S. W. Kuo, *Polymer* **2022**, *254*, 125070.

SUPPORTING INFORMATION

Additional supporting information can be found online in the Supporting Information section at the end of this article.

How to cite this article: M. Ejaz, M. G. Mohamed, W.-C. Chang, S.-W. Kuo, *J. Polym. Sci.* **2024**, *62*(8), 1629. https://doi.org/10.1002/pol.20230174